ADVANCED FUNCTIONAL MATERIALS
www.afm-journal.de

Transfer Printing of Cell Layers with an Anisotropic Extracellular Matrix Assembly using Cell-Interactive and Thermosensitive Hydrogels

*Indong Jun, Seok Joo Kim, Ji-Hye Lee, Young Jun Lee, Young Min Shin, Eunpyo Choi, Kyung Min Park, Jungyul Park, Ki Dong Park, and Heungsoo Shin**

The structure of tissue plays a critical role in its function and therefore a great deal of attention has been focused on engineering native tissue-like constructs for tissue engineering applications. Transfer printing of cell layers is a new technology that allows controlled transfer of cell layers cultured on smart substrates with defined shape and size onto tissue-specific defect sites. Here, the temperature-responsive swelling-deswelling of the hydrogels with groove patterns and their versatile and simple use as a template to harvest cell layers with anisotropic extracellular matrix assembly is reported. The hydrogels with a cell-interactive peptide and anisotropic groove patterns are obtained via enzymatic polymerization. The results show that the cell layer with patterns can be easily transferred to new substrates by lowering the temperature. In addition, multiple cell layers are stacked on the new substrate in a hierarchical manner and the cell layer is easily transplanted onto a subcutaneous region. These results indicate that the evaluated hydrogel can be used as a novel substrate for transfer printing of artificial tissue constructs with controlled structural integrity, which may hold potential to engineer tissue that can closely mimic native tissue architecture.

1. Introduction

A number of biodegradable scaffolds based on synthetic or natural polymers have been widely used in the regeneration of damaged tissues.[1] They serve as an artificial extracellular matrix (ECM) by providing mechanical support to which cells may adhere and direct cellular function.[2] Ideally, the degradation kinetics should be coordinated with the rate of neo-tissue formation; however, the uncontrolled degradation of scaffolds may suppress the migration of cells or provide insufficient mechanical integrity, leading to incomplete restoration. In addition, chronic inflammatory responses have often been observed due to changes in local pH caused by acidic degradation by-products, which may damage transplanted cells within the scaffolds and the surrounding host tissues.[3]

An alternative to the use of biodegradable scaffolds may involve harvesting single or multiple cell layers (cell sheets) with intact ECM assemblies, which can be subsequently transplanted without scaffolds.[4] While conventional methods use chelating agents and digestive enzymes in the collection of single cells, a cell layer can be obtained by physical detachment without disruption of cell-ECM or cell-cell junctions by the use of temperature-responsive polymers, magnetic nanoparticles,[5] or polyelectrolytes (voltage, surface polarization).[6,7] The most popular approach is the use of tissue culture poly(styrene) (TCPS) dishes covalently grafted with temperature-responsive poly(*N*-isopropyl acrylamide) (PIPAAm).[8] Cells can be attached to PIPAAm-grafted TCPS and cultured until confluence at 37 °C, and the grafted polymer chains become hydrophilic and freely extended at 20 °C, allowing confluent cell layers to spontaneously detach from the dish without the need for trypsin. The transplantation of cell sheets generated from different cell sources has been applied to several *in vivo* animal models (or clinical trials), resulting in improved tissue regeneration in the heart, cornea, liver, and esophagus.[9–11]

It has been reported that each type of tissue in the body presents distinct structural differences, which play an important role in function. For example, skeletal muscle tissue consists of parallel bundles of multinucleated myotubes that allow the propagation of electrical and mechanical signals, and ventricular myocardium is a quasi-lamellar tissue in which cardiac muscle fibers are hierarchically surrounded by bundled collagen sheaths with a honeycomb-like structure, which regulates synchronized contractile movement.[12] Therefore, several attempts have been

I. Jun, S. J. Kim, J.-H. Lee, Y. J. Lee, Y. M. Shin
Prof. H. Shin
Department of Bioengineering
Hanyang University
17 Haengdang-dong, Seongdong-gu,
Seoul 133-791, Republic of Korea
E-mail: hshin@hanyang.ac.kr
E. Choi, Prof. J. Park
Department of Mechanical Engineering
Sogang University
Sinsu-dong, Mapo-gu, Seoul 121-742, Republic of Korea
K. M. Park, Prof. K. D. Park
Department of Molecular Science and Technology
Ajou University
5 WonChun-dong, Yeoungtong-gu, Suwon 443-749, Republic of Korea

DOI: 10.1002/adfm.201200667

made to recapitulate native tissue structures using biomaterials. In particular, advances in microprocessing techniques have made it possible to prepare substrates with micro or nanoscaled patterns including aligned electrospun fibers,[13] microgrooved membranes,[14] nanopatterned tissue culture plates,[15] and poly(dimethylsiloxane) (PDMS) with symmetrical order of nanopits.[16] When cultured on these patterned substrates, cells can sense underlying geometrical cues, showing modulated cellular activities similar to those found in a native structural microenvironment; however, many of these materials are only applicable as in vitro model systems. Although transplantable in clinical applications, the aforementioned problems such as unexpected degradation and inflammatory response, may occur. Meanwhile, cell sheets with defined structural organization created using a PIPAAm-based surface have also been investigated. Examples include the selective and patterned polymerization of PIPAAm monomers using electron beam irradiation,[17] microtexture formation by hot embossing,[18] PIPAAm-grafted surfaces with microcontact-printed protein patterns,[19] and site-selective grafting of hydrophilic copolymers.[20] Although patterned cell sheets have been achieved from fibroblasts, hepatocytes, endothelial cells, and smooth muscle cells, the approaches listed above generally involve multiple-step processes. Microtextures were generated on the surface of TCPS, which was further grafted with PIPAAm. Microcontact printing of ECM proteins also has drawbacks concerning stamp deformation, ink (protein) diffusion, and the stability of patterns. The use of recombinant or animal-originated ECM proteins may cause an immune response upon implantation of a cell sheet. In addition, the uncontrolled grafting of PIPAAm on a rough surface and the removal of un-reacted monomer and chemicals may negatively affect cell sheet formation, as it has been reported that cells are sensitive to the thickness of a grafted PIPAAm layer.

The thermorheological studies with aqueous solutions of Tetronic, tetrafunctional tri-block copolymer of poly(ethylene glycol)-*co*-poly(propylene oxide)-*co*-poly(ethylene oxide) (PEO-PPO-PEO), have previously demonstrated an abrupt increase in their viscosity with increase in temperature within the range from 20 °C to 30 °C, and Tetronic-based hydrogels also showed thermosensitive behavior between 37 °C and 4 °C.[21,22] Despite interesting properties of Tetronic, there has been no study to harvest cell layers with ECM assembly because of their intrinsic non-fouling property leading to limited cell adhesion.[23] Recently, we have synthesized cell-interactive hydrogels from tyramine-modified Tetronic in which the cell-adhesive peptide (Arg-Gly-Asp) was readily incorporated into the hydrogel during crosslinking reaction.[24,25] In this study, combining multifunctionality of the synthesized Tetronic-based hydrogels and microfabrication technology, we present their versatile and simple use as a template to harvest cell layers with anisotropic ECM assembly.

2. Results and Discussion

2.1. Preparation of Cell-Interactive and Thermosensitive Hydrogels with Micropatterns

Figure 1 illustrates the fabrication scheme of thermosensitive hydrogels incorporated with a cell-interactive peptide and micro-scaled anisotropic groove patterns (25 μm) for transfer printing of cell layers. Each compartment of the dual syringe contained the same concentrations of Tetronic–tyramine (Tet–TA) as was synthesized previously.[24] Upon extrusion, the components A [polymer, a peptide, and horseradish peroxidase (HRP)] and B (polymer, and H_2O_2) were mixed, infused between a PDMS mold and glass plate, and spontaneously cross-linked within several minutes by the catalytic oxidation/reduction of H_2O_2/HRP. As depicted in Figure 1b, we hypothesized that 1) cells are attached on patterned hydrogels and cultured to form a confluent layer at 37 °C while integrin receptors bind to the peptide presented from the hydrogel and 2) the cell layer can be easily transferred to any substrate without the disruption of cell-cell junctions as the size of the thermosensitive hydrogels are enlarged in response to temperature transition (to 4 °C). Given that, the hydrogel must be possessed with adequate patterned features, support the formation of cellular assembly guided by underlying patterns, and allow size transition under biologically non-toxic conditions.

The presence of the peptide and micropatterns was confirmed by fluorescence and phase contrast microscopy, respectively. The

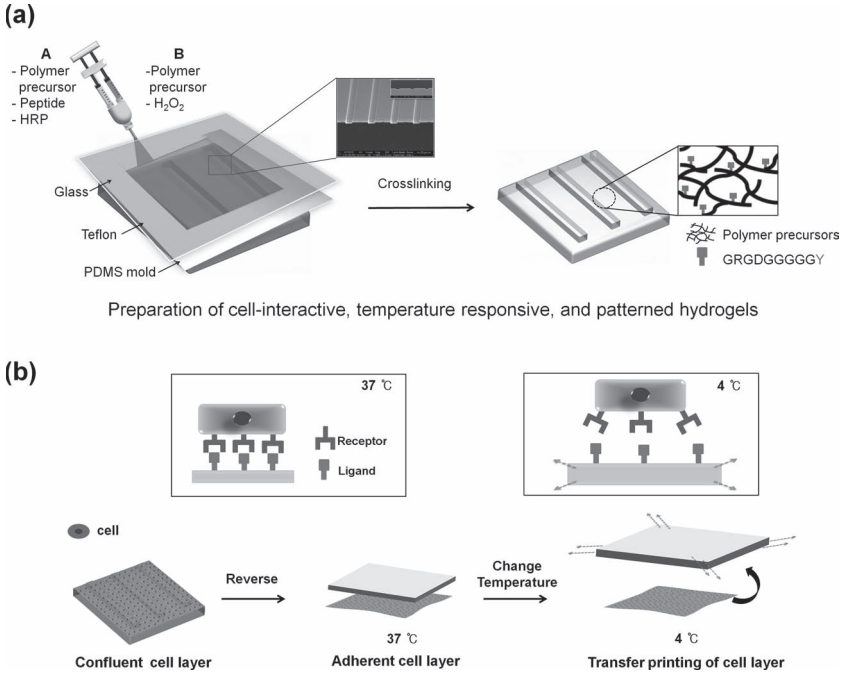

Figure 1. Schematic illustration of a) preparation of cell-interactive and thermosensitive hydrogels with anisotropic groove patterns and b) transfer printing of a cell layer cultured from the hydrogels by changing the temperature from 37 °C to 4 °C. The hydrogels are expanded at 4 °C as indicated by the dashed arrows and the binding between the cell membrane receptors and the hydrogel ligands is disrupted while the cell-cell junctions are maintained.

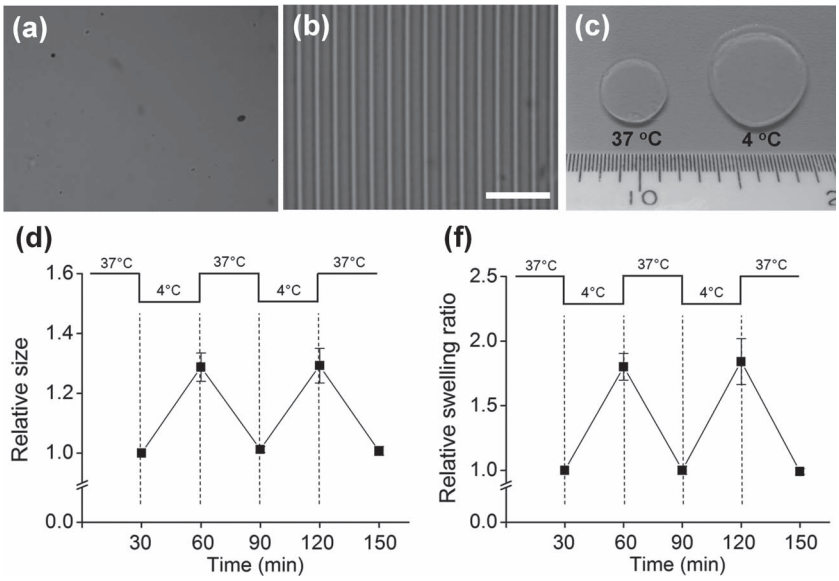

Figure 2. Surface morphology of hydrogels: phase contrast images of a) unpatterned and b) patterned hydrogels. Temperature-responsive characteristics of hydrogels: c) macroscopic image of hydrogels at corresponding temperatures and reversible changes in d) size and e) swelling ratio of hydrogels in PBS in response to alteration of temperature between 37 °C and 4 °C. Scale bar in (b) represents 100 μm and ruler in (c) indicates centimeters.

surface of the unpatterned hydrogels was smooth and flat, while uniform anisotropic micropatterns whose features were correlated to those of the PDMS molds (25 μm: groove, 10 μm: ridge) were created on the surface of the patterned hydrogels, as shown in **Figure 2**. The incorporated peptide was homogeneously distributed throughout the hydrogel surface regardless of the presence of patterns (see Supporting Information Figure S1). We previously showed that enzymatic crosslinking of Tet–TA is beneficial for the in situ incorporation of bioactive molecules with tyrosine groups that can be covalently linked to three-dimensional (3D) hydrogels via a one-pot reaction.[24,25] Various chemistries have been reported to generate biofunctional hydrogels, but acrylate group-based photopolymerization has been the most widely investigated method to create topographic patterning on the surfaces of hydrogels.[26] The major drawback to this process is that the bioactive protein or peptide should be acrylated before being incorporated, which can be avoided in our enzyme-triggered reaction. The concentration of H_2O_2 (0.05 wt%) is non-cytotoxic when polymerized with cells. The concentration of catalyst modulates the gelation time, which is an important factor for the elimination of defects in patterns such as roof collapse or buckling. The patterns were formed homogeneously throughout the surface under the aforementioned conditions. The concentration of peptide was fixed at 2.0 mg mL^{-1}, a level that supported adhesion and the proliferation of myoblasts.[24]

We then characterized the swelling behavior and size changes of the hydrogels in response to temperature changes. We preheated the samples to 37 °C and subsequently incubated them at 4 °C for 30 min, and this cycle was repeated at least three times; we then measured the swelling ratio and size of the hydrogels. As shown in Figure 2d, when the temperature cooled from 37 °C to 4 °C, the relative size and swelling ratio of hydrogels were increased to 1.29 ± 0.06 and 1.84 ± 0.18, respectively. The transition of hydrogel properties was reversibly maintained when the temperature in the incubator was repeatedly alternated, as shown in Figure 2d–e. The thermoresponsive phenomenon has been widely observed for many polymers such as PIPAAm, methylcellulose, and Pluronic, and is attributed to the self-assembly of hydrophobic or hydrophilic domains within a distinct temperature range.[27–29] The Tet–TA-based hydrogel possesses four polymeric arms composed of long chains of poly(ethylene oxide) (PEO) and poly(propylene oxide) (PPO). At 37 °C, PPO chains may be arranged to contribute tight hydrophobic interactions that decrease the size of the hydrogel, while the hydrophilic binding between PEO domains may be dominant at 4 °C, leading to increased hydration, as shown in Figure 2c. It should be noted that these thermosensitive characteristics were maintained after a crosslinking reaction over the temperature range relevant to biological environments. The hydrogel may undergo a transition from hydrophobic to hydrophilic interactions above 4 °C; however, 4 °C was chosen for the experiment to maximize an increase in size without causing critical damage to cells.[30,31]

2.2. Temperature-Dependent Cell Layer Transfer

To probe the transfer of a cell layer from the hydrogel in response to temperature change, C2C12 myoblasts were cultured on the patterned hydrogels and allowed to attach overnight. They became confluent and elongated along the direction of the patterns on the hydrogels (**Figure 3**). Interestingly, they were able to span the distance between ridges (10 μm wide). When the temperature was lowered to 4 °C, the confluent cell monolayer was spontaneously detached from the hydrogel in the absence of digestive enzyme. Complete detachment was achieved by incubation for 10 min. In order to investigate the transfer print of the cell layer, the cells cultured on the hydrogels were overlaid on a glass plate, which was incubated at 4 °C for 10 min to allow the cell layer to transfer and attach to the new surface. We fabricated a square-shaped hydrogel, and the corresponding size and shape of cell layer was harvested on the glass surface after transfer (Figure 3c). The cells were completely detached from the hydrogel as a tissue-like construct, and no remaining cells were observed following the transfer (Figure 3d). The myoblasts cultured on the glass and alginate hydrogels incorporated with the same type of peptide sequence, which were incubated under the same conditions, showed no detachment even after prolonged incubation (data not shown).

The use of thermosensitive polymers, magnetic cationic liposomes with magnetic particles, polyelectrolyte surfaces, and cationic peptide detergents have been reported to facilitate the harvesting of cell layers without employing chelating agents or

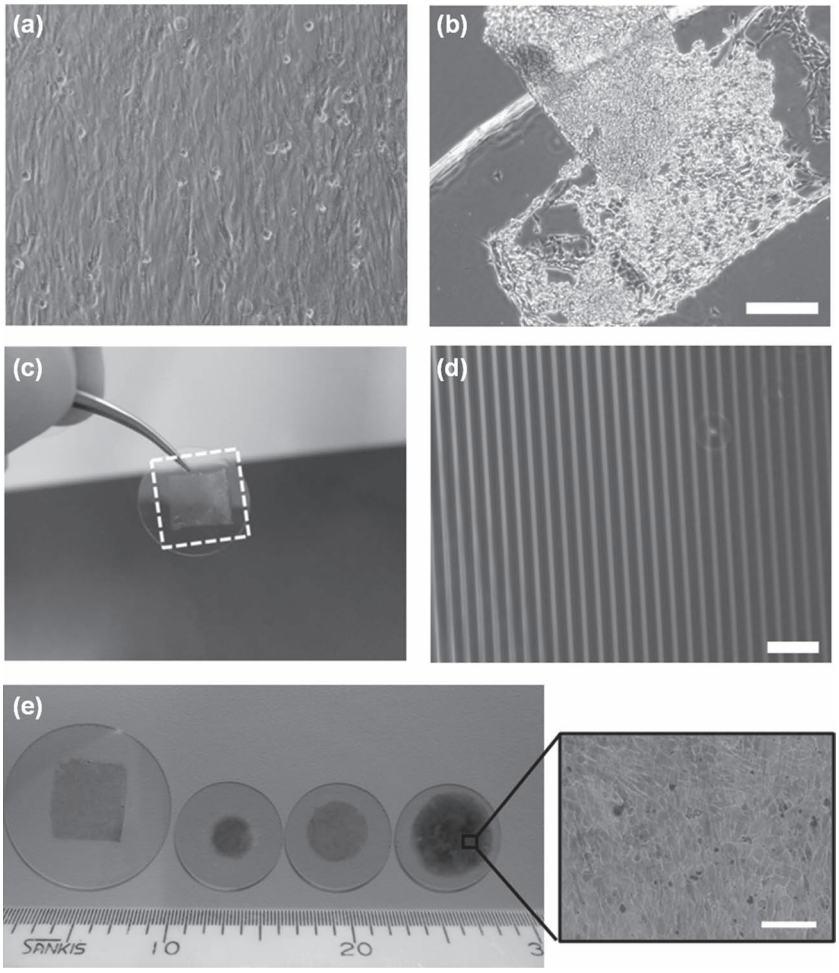

Figure 3. Detachment and transfer printing of myoblast layers cultured on thermosensitive hydrogels by reducing the temperature from 37 °C to 4 °C. a) Morphology of myoblasts densely cultured on the patterned hydrogels at 37 °C. b) Detachment of the myoblasts from hydrogels at 4 °C after 5 min of incubation. c) Macroscopic view of a cell layer transferred to a glass substrate by temperature transition (from 37 °C to 4 °C). d) A phase contrast image of hydrogels after transfer printing of tissue, suggesting the complete transfer of the cell layer from the hydrogels. Transfer printing of cell layers from hydrogels of several sizes and shapes to various substrates: e) transferred cell layers on glass prepared from hydrogels with rectangular and circlular shapes of different diameter (8, 12, 15 mm). Scale bar represents 100 μm.

digestive enzymes,[32,33] but the most popular approach relies on a thermo-responsive substrate.[10,31] PIPAAm is covalently grafted on the surface of a regular polystyrene cell culture dish on which cells can be cultured to reach confluency at 37 °C. However, cells can be detached while maintaining cell-cell junctions by lowering the culture temperature to 20 °C, below LCST, which changes the configuration of the grafted PIPAAm chains to produce a hydrophilic surface. In this approach, the transfer of cell layers is influenced by the grafting density and chain length of the polymerized PIPAAm on the surface. It has been reported that a graft yield less than 40% was unlikely to be sufficient to permit the disruption of cell adhesion to the substrate, and a 50% graft density also led to poor recovery of intact cell-cell junctions.[18] In our system, the transfer of cell layers is facilitated by a change in gel volume induced by a lowered temperature, which seems to be a critical factor to induce the detachment of cells. It would be worthwhile to investigate the effects of the degree of crosslinking on the successful transfer of cell layers.

We then examined whether we were able to control the shape of the transferred cell layer on the glass. We simply prepared the hydrogels with different sizes of circular shapes (8, 12, or 15 mm in diameter), as shown in Figure 3e, and the various shapes and sizes of the cell layer were readily transferred onto the glass plate. After transfer, the confluent cells with intact cellular contacts were positively stained with hematoxilin, and no defects or void spaces free of the cell layer were observed. It should be noted that cells could be cultured on the hydrogels of various sizes or shapes until confluency, and that the dimensions and geometries of the transferred cell layers completely coincided with the original ones. As alternative substrates, poly(L-lactide-*co*-caprolactone) (PLCL) and poly(L-lactide) (PLLA) were used to generate film by the solvent casting method and aligned nanofibers by electrospinning, respectively (see Supporting Information Figure S2). We observed that the cell layers were transferred onto both types of synthetic polymer substrates and stably readhered to them, as observed on the glass plate. These results are promising in that we could simply stack multiple layers of cells on the tops of cells cultured on tissue-engineered scaffolds. These cells may have distinct properties, which may control cell-cell communications similar to that of the native cellular microenvironment in the human body when cultured as double or multiple layers transferred by our hydrogels. In addition, our approach may be complemented with a conventional cell sheet harvest technology that requires a supporting PVDF transfer membrane or protein-coated plunger for transplantation,[34,35] while we can directly transfer artificial tissue constructs with defect-specific sizes and shapes from custom-made thermosensitive hydrogels, as shown in our proof-of concept experiments.

2.3. Transfer Printing of Patterned Cell Layers

We analyzed the adherent morphology and cytoskeletal structure of the myoblasts as cultured on hydrogels and how they are affected by the transfer process using phase contrast and immunofluorescence microscopy. As shown in **Figure 4**a–d, the phsase contrst microscopic images revealed that the majority of the myoblasts on the patterned hydrogels exhibited dense cell-cell contact network formations oriented to the direction of patterns on underlying hydrogels, while they were randomly oriented on the unpatterned hydrogels. The elongated myoblasts

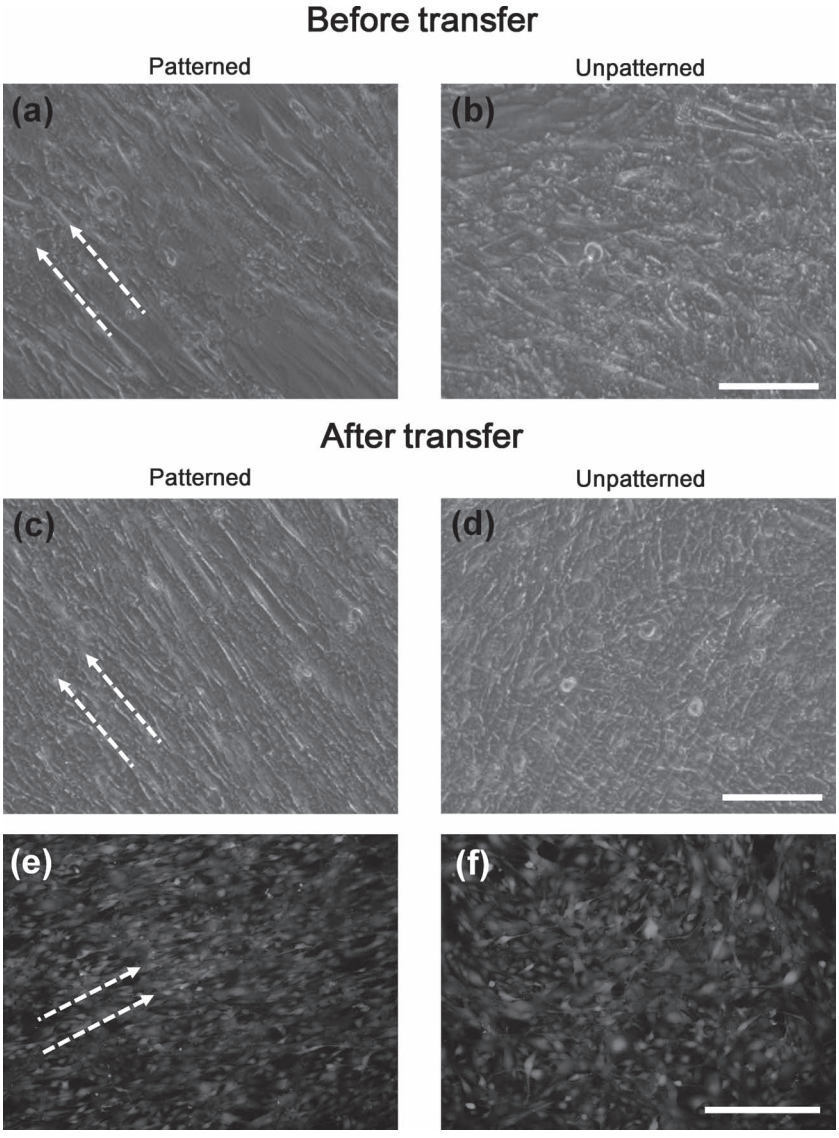

Figure 4. a,b) Phase contrast images of myoblasts cultured on patterned and unpatterned hydrogels. c,d) Images of myoblasts on the glass after transfer printing. e,f) Representative images of myoblasts indicating live and dead cells after transfer printing (only few dead cells were observed). Arrows in (a,c,e) indicate the direction of micropatterns. Scale bars indicate 100 μm for (a–d) and 200 μm for (e,f).

longitudinally oriented to the direction of patterns (as indicated by arrows) were packed to each other resulting in confluent monolayer before transfer printing process. It was confirmed that these structural differences were maintained after the cells were transferred to the glass plates. We then investigated the effect of transfer condition on viability of myoblasts. Figure 4e,f show monolayer of cells transferred on the glass, which were treated with calcein AM and ethidium homodimer-1. Cells were aligned as seen in phase contrast images and appeared to be viable throughout the surface with only few dead cells. In this study, we selected the temperature of 4 °C for transfer printing. Although commonly used temperatures for obtaining cell sheets are 20 °C and 37 °C, several studies have been performed at 4 °C and demonstrated no detrimental outcome to the cells. Most importantly, we selected a relatively short incubation time (within 10 min) and observed no shrinkage or fragmentation of the cells during the process. Collectively, these results suggest that our process had no critical damge on cells for practical applications.

Fluorescence staining for paxillin (one of representative structural and functional proteins involved in formation of focal adhesion in anchorage dependent cells) reconfirmed the anisotropic arrangement of densely cultivated cell monolayers, which were maintained before and after transfer processes as shown in **Figure 5**a,b. We then measured the orientation degree and nuclear aspect ratio from the fluorescent images. (see Supporting Information Figure S3) Quantification analysis showed no significant differences in the orientation degree or aspect ratio among the groups analyzed before transfer and those analyzed after transfer, as shown in Figure 5c,d. The average orientation degree was less than 15° (12.63° ± 7.63°) relative to the original direction of the patterns on the hydrogels, while this value was more arbitrary on the unpatterned hydrogels (46.89° ± 25.04°). No significant differences were observed after transfer, indicating that the patterned cellular assembly can be transferred. The same trend was found for the nuclear aspect ratio, in which the values were significantly different between the patterned (0.59 ± 0.07) and unpatterned hydrogels (0.79 ± 0.10) both before and after the transfer. We then cultured the transferred cell layers on the glass plate for three additional days. During this culture period, the orientation and alignment of cells were continuously maintained in the absence of structural guidance from the underlying substrates. Despite the lack of a statistically significant difference, the variations in the orientation degree and nuclear aspect ratio increased after three days. This may be due to a reorganization of cellular assemblies in the absence of a substrate pattern.

We also studied filamentous actin formation (F-actin) and fibronectin (FN) expression (mainly produced from myoblasts) in the transferred cell layers. The stress fibers and fibrillar structure of FN showed preferential alignment parallel to the direction of the micropatterns, while they were randomly distributed on the cell layer transferred from the unpatterned hydrogels as shown in **Figure 6**a,b. (see Supporting Information Figure S4 for enlarged images) The morphology of myoblasts is essential for differentiation into myotubes to form organized structures since skeletal muscle is composed of assembled fibers formed from multinucleated myotubes. Our results suggest that the hydrogel may be effective for modulation of myogenic differentiation of myoblasts, and the transferred cell layers retained

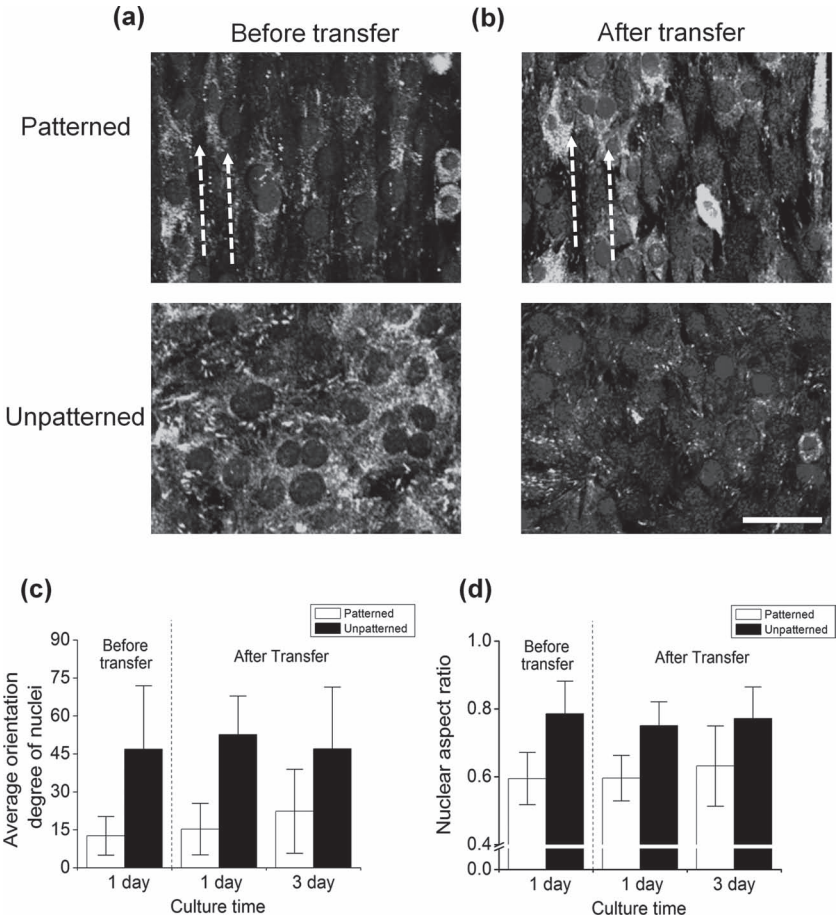

Figure 5. Immunofluorescence images of myoblasts on the hydrogel before transfer printing and dashed lines are direction of patterns. a) Myoblasts on patterned and unpatterned hydrogels where cells were stained for paxillin and nuclei. b) Images are from myoblasts on the glass after transfer printing. Analysis of characteristics of the transferred cell layers: c) average orientation degree of nuclei and d) aspect ratio of cells on the hydrogels and glass plate, before and after transfer. Myoblasts were cultured for one day on the thermosensitive hydrogels, transferred onto the glass plate by reducing the temperature, and cultured for three additional days. Scale bar represents 50 μm.

the oriented structures and associated ECM. Various technologies to create tranferrable cell layers with a distinct structural organization have been described, with a combination of micro/nano manufacturing and chemical modification being widely utilized. Initial work has involved a hot embossing approach, in which microsized line patterns were generated on the surface of polystyrene (PS) by pressing a PDMS mold against a PS plate, followed by PIPAAm grafting onto the PS.[18] Microcontact printing of a protein (e.g., FN) on the PIPAAm-grafted PS and the seeding of cells under serum-free media were successful, allowing the formation of cell sheets with defined structural organizations.[19] Recently, a hydrophilic block copolymer containing poly(N-acryloylmorpholine) segments was custom-synthesized and selectively grafted onto the defined regions with strip patterns that prevent cell adhesion.[20] Although cell layers that can be transferred with organized cellular assemblies have been achieved by the abovementioned techniques, some drawbacks still remain that allow room for the development of improved methods. A microtextured surface can be created on a PS substrate with reasonable resolution (over micrometer scale); however, this requires multiple complex steps, and the homogeneous graft-polymerization of PIPAAm may not be guaranteed. Microcontact printing is an inexpensive technique to precisely control cell shape; however, complete printing on a PIPAAm-grafted surface may be difficult (the size of a PDMS stamp is usually smaller than the substrate area), leaving an unpatterned periphery. It also requires the avoidance of sophisticated chemical reactions for synthesis and the selective grafting of complex polymer brushes. In contrast, for thermosensitive Tet–TA-based hydrogels, any patterns with microsized topography may potentially be generated with PDMS molds in a one-pot process and in a reproducible manner. The patterns are sufficiently stable for the long-term culture of therapeutic cells, and, more importantly, crosslinking utilizes a phenol functional group. Thus multiple types of peptides or proteins with tyrosine can be easily incorporated within the hydrogel.

We then investigated the effects of pattern on the formation and retention of aligned myotubes. We harvested the cell layer that was further incubated in the myogenic differentiation media for two additional days after transfer and stained for myosin heavy chains. In agreement with the abovementioned results, Figure 6c,d show that myotubes appeared to be organized along the direction of the micropatterns, while they were randomly distributed on the cell layer transferred from the unpatterned hydrogel. The orientation degree of the myotubes was within 10° of the direction of the long axis (> 85%). In contrast, the average orientation degree was 35.67° ± 20.65° on a cell layer transferred from the unpatterned hydrogels as shown in Figure 6e,f. Myoblasts should form multinucleated myotubes during the differentiation process, as they are important for synchronized contractile movement.[36] There have been intensive reports with unique substrates, including unisotropic patterned electrospun fibers,[37] patterned PDMS substrates,[38] and self-assembled matrix monolayers,[39] demonstrating that anisotropic structures from the underlying matrix enhance the aligned myotube formation and accelerate the myogenic differentiation of myoblasts. Although a two-dimensional substrate enables the controllable differentiation of myoblasts and anisotropically assembled myotube formation, their manipulation is necessary for the application of engineered organized cell/tissue constructs to regenerate tissue. Our results suggest that the hydrogel supports the alignment of cells and the robust formation of highly dense cell-cell junctions preferentially oriented to the direction of the underlying patterns, which can be directly transferred to the desired sites. Furthermore, it seems fair to conclude that the transferred cell layer may memorize

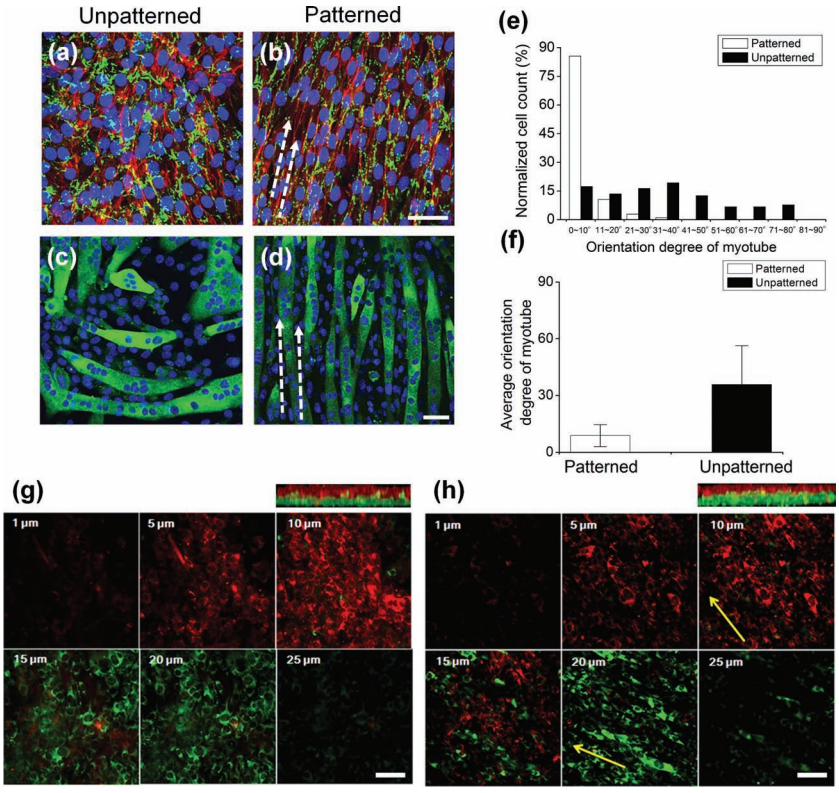

Figure 6. Cytoskeletal structure and ECM distribution on myoblasts cultured on a) unpatterned and b) patterned hydrogels. The images were obtained by immunofluorescence staining for fibronectin (green) and F-actin (red) on the cell layer 24 h after transfer printing. Immunofluorescence images stained for sarcomeric myosin heavy chain from transferred cell layer cultured on c) unpatterned and d) patterned hydrogels. e) Histogram of orientation and f) quantification of average orientation degree of myotubes. Multilayered tissue constructs on glass were prepared by the transfer printing of multiple cell layers. To visualize the multilayered structure, the top and bottom layers were stained with cell-tracker red and green dyes, respectively, and analyzed using confocal laser scanning microscopy. g) Orthogonal images of multiple layers; each image was captured at depth intervals of 5 μm. Each layer was prepared from unpatterned hydrogels. h) Orthogonal images of multiple layers of cells originally cultured on the patterned hydrogels; each image was captured at depth intervals of 5 μm. Arrows represent the direction of the patterns. Scale bars represent 100 μm for (a–d) and 200 μm for (g,h).

the structural integrity guides from the underlying matrix and maintain and affect the differentiation of myoblasts despite transfer onto any substrate.

2.4. Manipulation of Multiple Cell Layers

We then examined the possibility of layering contiguous cell layers. The primary cell layer was harvested on the glass by lowering the temperature to 4 °C for 10 min and another hydrogel with a confluent cell layer was overlaid on the harvested bottom layer and incubated for additional 10 min. By repeating this procedure, multiple cell layers were stacked, resulting in quadruple-layer tissue constructs (Figure 6g,h). Orthogonal confocal laser microscopy images exhibited the highest intensity from Vybrant DiD (red)-labeled myoblasts at 10 μm from the top layer, which was mixed with Vybrant™ DiO (green)-labeled cells at 15 μm. All cells were green at a depth of 20 μm, with clear separation between the green and red labeling in a vertical view. There was a similar trend when cell layers harvested from patterned hydrogels were stacked. The stacking process had no effect on the organization of cellular assembly; the distinct direction of each aligned cell layer that is indicated by yellow arrows in Figure 6h was clearly observed at each layer in the orthogonal images, suggesting that multilayered tissue constructs could be deposited successfully with patterned and unpatterned hydrogels. (see Supporting Information Figure S5 for enlarged images) Previously described methods to create multiple transferred cell layers often required at least two steps: a cell layer is transferred to fibrin or a gelatin-coated manipulator and is then re-transferred onto new substrates.[4,18,20]

Our method may be simpler and more facile for manipulating stacked cell layers with desirable sizes in a one-step process. No strategies have been proposed to appropriately regenerate complex 3D tissue structures with multiple cell populations (e.g., myocardium that is composed of muscle fibers and organized ECM or a blood vessel with three distinct layers). The ability to reconstruct 3D structures with oriented cells/ECM assemblies using thermosensitive hydrogels should be highlighted to address these technical challenges. In addition, our system can be used to identify regulatory mechanisms in basic biology. It has never been satisfactorily explained how the cross-striated patterns of layered muscular tissue affect its contractile functions, which may be answered by fabricating stacked layers of myoblasts arranged with diverse orientations.

2.5. Subcutaneous Transplantation of Tissue Constructs from Hydrogel Cultures

To rapidly demonstrate whether desirable cells could be transplanted in vivo as a layer, we established a subcutaneous graft model. As shown in **Figure 7**, a cell layer containing approximately 8×10^4 to 1.2×10^5 myoblasts was successfully transplanted onto subcutaneous skin. From a cell therapy perspective, the retention of transplanted cells at the defect site is an important criterion in regeneration.[40,41] Therefore, a cell layer transplanted using our system will have potential for the regeneration of target tissue. H&E staining showed that there was minimal evidence for recruiment of multinucleated inflammatory cells to the transplanted tissue although it was hard to pin point the location of the cell layer. To confirm the presence of the tissue construct between native tissues, we pre-labeled a cell layer before transplantation, which was

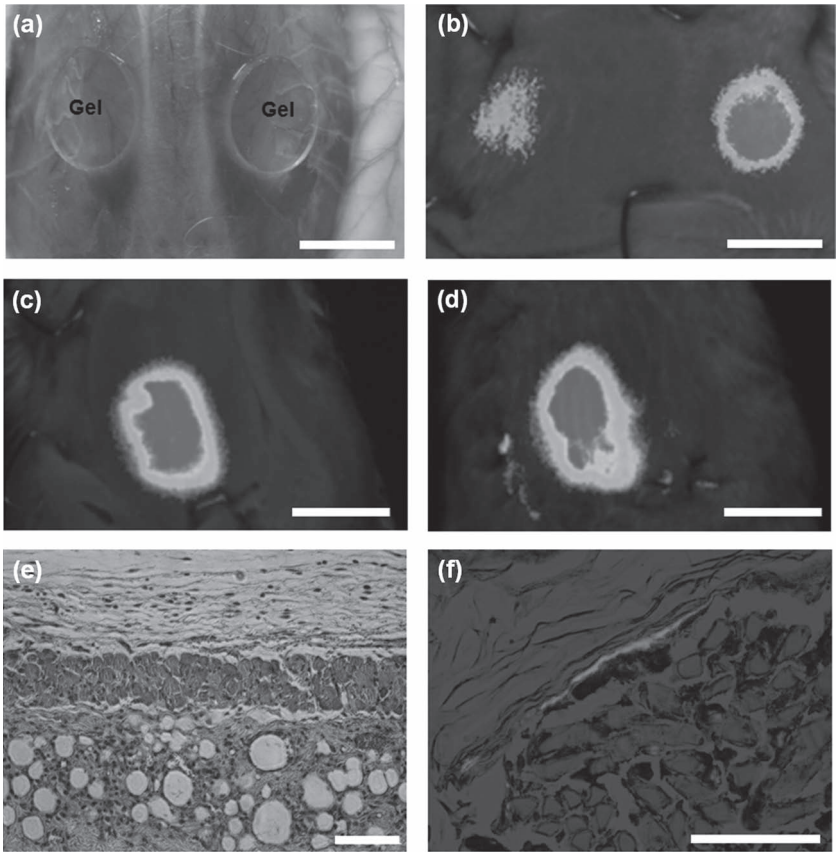

Figure 7. Direct transplantation of a cell layer by transfer printing technique. a) Macroscopic view of transplanted hydrogels on subcutanous tissue. For visualization, myoblasts were pre-labeled with a cell-tracker before being cultured on the thermosensitive hydrogels. b) Transfer tissue construct on subcutaneous skin for 5 min (left) and 30 min (right). Square-shaped tissue construct was transferred to native tissue, and cell retention was observed at c) 0 and d) 6 days. Scale bar is 8 mm. Histological analysis of myoblast-based tissue constructs with e) hematoxylin and eosin staining and f) dystrophin staining and fluorescent detection of transplanted tissue constructs (a white thin layer in the middle of the figure). Scale bar represents 100 μm.

found in the histological section with positive staining for dystrophin, suggesting potential muscle regeneration within the implanted region. Although there are many approaches to the regeneration of a tissue defect using cell sheets, they require a minimum of two steps: the cell sheet transfer to PVDF or fibrin gel and re-transfer to the tissue defect site.[42–44] In contrast to these approaches, the transfer printing of the tissue method has many advantages over the previously reported methods. First, the fabrication of cell-interactive hydrogels with structural patterns is simple and fast. Second, the developed hydrogels can be manufactured by custom-made sizes or shapes that will be ultimately regenerated as the target tissue. Third, the tissue-construct is simply transferred onto the tissue defect site in one step by temperature transition. Although we showed our proof-of-concept study that patterned layer can be easily transferred to the subcutaneous tissue under defined transfer condition, we are still in progress in developing animal models and experimental techniques to clearly investigate in vivo efficacy of our system in regeneration of tissue with structural relavance to cell layers with anisotropic ECM assembly.

3. Conclusions

In this study, we developed thermosensitive hydrogels with a cell-adhesive peptide and microscaled anisotropic groove patterns via bio-inspired enzymatic polymerization. We then evaluated the feasibility of these hydrogels as a substrate to create a tranferrable cell layer using temperature changes. Our results showed that the cell layer can be easily transferred to new substrates by lowering the temperature from 37 °C to 4 °C for 10 min. Moreover, the anisotropic patterns of the assembled cells and ECM were also transferrable and the orientation of myotubes was aligned with the pattern direction. In addition, we successfully stacked multiple cell layers on the new substrate in a hierarchical manner, and the cell layer was easily transplanted onto a subcutaneous region, where it was retained for more than six days. Collectively, we present a novel transfer printing approach to create a cell layer with anisotropically assembled ECM using a synthetic thermoresponsive hydrogel, which can be utilized to regenerate target-specific tissues.

4. Experimental Section

Preparation of Micropatterned Cell-Adhesive Hydrogels: Micropatterned cell-adhesive hydrogels were prepared using a PDMS mold, in which microscale grooves (10 and 25 μm for ridge and groove, respectively) were patterned by conventional photolithography techniques using a positive photoresist (AZ7220, AZ Electronic Materials Ltd., Branchburg, NJ, USA). The patterned microscale grooves were etched by deep reactive ion etching (DRIE), and the photoresist layer was removed. The final depth of DRIE was 2 μm, and the fabricated wafer was used as a master for PDMS (Sylgard 184 Silicone Elastomer, Dow Corning, Midland, MI, USA) replica molding. The mixture of PDMS and a curing agent (10:1 ratio) was then poured over the fabricated wafer and cured on a hotplate at 95 °C for 1 h. The peeled-off PDMS mold was serially rinsed with acetone, isopropyl alcohol, and deionized water and completely dried prior to use. Two discrete Tetronic-tyramine polymer solutions (7% (w/v)) were prepared in 1) phosphate buffered saline (PBS) with H_2O_2 (0.05 wt%) and 2) in PBS with HRP (0.025 mg/ml) and the cell-adhesive peptide (GRGDGGGGGY, 2.0 mg mL^{-1}), which were separately loaded into a dual syringe as shown in Figure 1. The polymer solutions were injected into the space between the PDMS mold and the glass plate, which were separated by 0.5 mm by a Teflon liner. The PDMS mold was coated with F-127 (2% w/v) before gelation so that the cross-linked hydrogels would easily detach from the mold. The cross-linked hydrogels were then washed three times with PBS and punched with differently sized or shaped borers (the circle shapes were 8, 10, and 15 mm in diameter, and the square shape was 10 mm per side). The shape of the micropatterned hydrogel surface was characterized using phase-contrast microscopy (CKX41, Olympus, Tokyo, Japan).

Characterization of Hydrogels: The incorporation of the cell-adhesive peptide on the surface of hydrogels was confirmed by fluorescein isothiocyanate (FITC) probe molecules; hydrogels were immersed in 1 mL of an FITC solution (2 mL mL^{-1} in EtOH) at room temperature for

3 h and serially washed with EtOH and PBS for 1 and 6 h, respectively. FITC can be conjugated to the terminal primary amine functional group in the peptide, and FITC-labeled hydrogels were visualized using a fluorescence microscope (Nikon TE-2000, Nikon Corp., Tokyo, Japan). The temperature-dependent changes in the size and swelling ratio of the hydrogels were measured by alternating the temperature four times from 37 °C to 4 °C. Hydrogel discs (diameter 10 mm) were immersed in 1 mL PBS and alternately incubated at 37 °C for 30 min and then 4 °C for 30 min. The size and weight of the swollen hydrogel discs were then recorded at each time point. The swelling ratio of the hydrogels was determined using following equation: swelling ratio = (Ws – Wi)/Wi, where Ws and Wi are the weights of the swollen hydrogels at 37 °C and at 4 °C, respectively.

Cell Culture and Transfer Printing of Cell Layers: C2C12 myoblasts (CRL-1772) (ATCC, Manassas, VA, USA) were cultured in Dulbecco's modified Eagle medium supplemented with 10% fetal bovine serum (FBS) and 1% p/s antibiotics under the standard culture conditions (37 °C, 5% CO_2), enzymatically lifted, and seeded on the hydrogels at a density of 1.5×10^5 cell/cm^2. C2C12 myoblasts were cultured on the hydrogels at 37 °C for 24 h to allow the cells to form a confluent monolayer. The emperature was then changed to 4 °C, and the cells were incubated for an additional 10 min. The detachment of the confluent monolayer was microscopically observed. Three types of substrates were prepared: film (8 wt% PLCL via solvent casting), glass and nanofiber (electrospun fibers, having diameters of ≈600–800 nm, spun using 6 wt% PLCL). For transfer, removed the media was removed and the hydrogels were overlaide on easch substrate and incubated at 4 °C for 10 min. The hydrogels were then pealed, media was added, and the cells at 37 °C were incubated to allow them to stably adhere to new substrates. Subsequently, the transferred cell layer on the new substrate were stained with Mayer's hematoxylin solution for 20 min and then washed with PBS to remove any non-specific staining.

Cell Viability After Transferred hMSC Layer Printing: For confirming viability of transferred myoblast layer, a Live/Dead viability/cytotoxicity kit (Molecular Probes, Eugene, OR, USA) was used immediately after the transfer process. Briefly, two component solution including calcein AM (1:1000) and ethidium homodimer-1 (1:500) were mixed, exposed to the cell layer for 30 min, and then imaged using a fluorescence microscope.

Immunofluorescence Staining: The cells on the hydrogels and those transferred to the glass by temperature changes were imaged using phase contrast and fluorescent microscopy (TE-2000, Nikon Corp., Tokyo, Japan). For immunostaining, the cells were fixed with 4% paraformaldehyde for 20 min and permeabilized with a cytoskeleton buffer (pH 6.8, 50 mM NaCl, 150 mM sucrose, 3 mM $MgCl_2$, 50 mM trizma-base, 0.5% Triton X-100) for 10 min. The permeabilized samples were treated with a blocking buffer (5% FBS in PBS) for 1 h, subsequently incubated with anti-paxillin (1:100) or anti-fibronectin (1:100) for 1 h, and then incubated with anti-mouse IgG biotin conjugate (1:100) and FITC-conjugated streptavidin (1:100) for 1 h. Cell nuclei and F-actin were counter-stained with Hoechst 33258 and rhodamine-phalloidin, respectively.

Measurement of Orientation Degrees and Aspect Ratios of Nuclei in Cell: Cell orientation was measured from fluorescent images of nuclei using Nikon image software (NIS-Elements AR, Nikon Corp., Tokyo, Japan). Nuclear staining was carried out with Hoechst 33258 on cells cultured on the hydrogel before the transfer and on those one and three days post-transfer. The perimeter of each nucleus was outlined, and lines designating long and short axes were drawn. The orientation degree of each individual nucleus was defined as the angle between the major axis of the ellipse-shape nucleus and the direction of the underlying pattern on the hydrogel. The aspect ratio of the nucleus was defined as ratio of the short axis to the long axis. For the quantitative analysis, 15 representative images per fluorescent image were scored (see Supporting Information Figure S3).

Differentiation of Myoblasts and Immunofluorescent Staining: At two days after cells were transferred and incubated with differentiation media, cells were immunostained for sarcomeric myosin and visualized by a fluorescence microscope. The cells were fixed, permeabilized, and blocked and then were sequentially incubated with MF20 (1:50), anti-mouse IgG biotin conjugate (1:100), and FITC-conjugated streptavidin (1:100). Cell nuclei and F-actin were counter-stained with Hoechst 33258 (1:5000) and rhodamine-phalloidin (1:200), respectively. Using a fluorescence microscope, 10 representative images per group were scored for myotube orientation by determining the degree of the long axis of the myotube. The values of 0° and 90° indicate anisotropic and isotropic myotube directions, respectively.

Fabrication of Multilayered Cell Sheets and Confocal Laser Scanning Microscopy: Confluently cultured cells on the hydrogel at 37 °C were gently placed over the glass and then incubated at 4 °C for 10 min to harvest a cell sheet on the glass. Next, the hydrogel was lifted from the glass, leaving the transferred cell sheet on the glass. In order to prepare a multilayered cell sheet, additional hydrogels with confluent myoblast cultures were overlaid on the cell sheet generated on the glass, and the same process was repeated to stack several layers of cell sheets (prepared four-layered cell sheets were prepared from patterned or unpatterned hydrogels). To visualize the multilayered tissue construct made of four cell sheets, cell tracker dyes were used to label the myoblasts. Specifically, confluent C2C12 myoblasts were pre-treated with Vybrant DiD (red) or Vybrant DiO (green) cell-labeling solutions for 30 min, sequentially enzymatically detached from TCPs using trypsin-EDTA, and seeded at 1×10^5 cell/cm^2 on each hydrogel. In this experiment, to easily identify each layer of the cell sheet, only the top and bottom layers were pre-labeled with the cell-labeling dye, but intermittent layers were prepared without labeling. These multilayered tissue constructs were then fixed in 4% paraformaldehyde and imaged using a confocal laser scanning microscope (CLSM) (LSM 5 EXCITER, Carl Zeiss, Oberkochen, Germany).

Subcutaneous Transplantation of Cell Layer with Controllable Shapes: It was confirmed that harvested cell layer can be transferred onto another tissue by changing temperature. Briefly, Balb-C mice (7 weeks old, male) were anesthetized with zoletil (50 μg/gram of mice), and their dorsal skin was sterilized using povidone-iodine-soaked gauze. After sterilization, cut the dorsal skin was cutin a "U" shape and immediately flipped the skin onto the mice's backs. All animals were treated in accordance with experimental procedures approved by Hanyang University (HY-IACUC-11-002). After C2C12 myoblasts were cultured on hydrogels for 24 h, the culture medium was removed and the hydrogels were moved onto the dorsal skin using tweezers. Once the hydrogels were placed on the dorsal skin, cool (4 °C) saline was periodically dropped onto the hydrogels for 10 min, then peeled the hydrogels from the skin. The incisions were closed with 5-0 nylon sutures, following the transplantation of the tissue constructs from the hydrogels. To confirm successful transfer of the tissue constructs from hydrogels with different shapes (8-mm-diameter circle and 5×10 mm rectangle), the cells were pre-labeled with DiD vibrant cell-labeling dye before being seeded onto the hydrogels. To observe the time-course of the transplanted tissue constructs labeled with dye, mice were anesthetized, and the intensity of the tissue constructs at a specific wavelength wsa analyzed using Image Station (4000MM, Eastman Kodak Company, Rochester, NY, USA). At five days after transplantation, the mice were euthanized, the skin flaps were removed, and a 20×20 mm section of dorsal skin was collected. Following these steps, the collected skin tissues were fixed with 4% paraformaldehyde solution for 24 h at room temperature. The tissues were rinsed with distilled water and prepared using the following steps for paraffin embedding: ≈70–100% EtOH, xylene, and paraffin. After these processes, sections were cut at a thickness of 4 μm with a microtome and stained them with hematoxylin and eosin and with dystrophin (Santa Cruz Biotechnology, Santa Cruz, CA, USA) as a muscle marker for immunohistochemistry.

Supporting Information

Supporting Information is available from the Wiley Online Library or from the author.

Acknowledgements

We acknowledge Dr. S. H. Do in Konkuk University for valuable discussion and assistance in histology and immunohistochemical analysis. This work was supported by the National Research Foundation of Korea(NRF) grant funded by the Korea government (No. 2011-0015222) and the Ministry of Education, Science and Technology (No. 2011-0007747).

Received: March 9, 2012
Revised: May 15, 2012
Published online: June 13, 2012

[1] T. Dvir, B. P. Timko, D. S. Kohane, R. Langer, *Nat. Nanotechnol.* **2011**, *6*, 13.
[2] M. P. Lutolf, P. M. Gilbert, H. M. Blau, *Nature* **2009**, *462*, 433.
[3] M. Lobler, M. Sass, C. Kunze, K. P. Schmitz, U. T. Hopt, *J. Biomed. Mater. Res.* **2002**, *61*, 165.
[4] T. Okano, N. Matsuda, T. Shimizu, M. Yamato, *Adv. Mater.* **2007**, *19*, 3089.
[5] M. Kamihira, H. Akiyama, A. Ito, Y. Kawabe, *Biomaterials* **2010**, *31*, 1251.
[6] J. Voros, O. Guillaume-Gentil, Y. Akiyama, M. Schuler, C. Tang, M. Textor, M. Yamato, T. Okano, *Adv. Mater.* **2008**, *20*, 560.
[7] T. Okano, Z. Tang, A. Kikuchi, Y. Akiyama, *React. Funct. Polym.* **2007**, *67*, 1388.
[8] H. E. Canavan, M. A. Cooperstein, *Langmuir* **2010**, *26*, 7695.
[9] T. Okano, *Tissue Eng.* **2007**, *13*, 1650.
[10] T. Okano, *Tissue Eng.* **2007**, *13*, 882.
[11] T. Okano, I. Elloumi-Hannachi, M. Yamato, *J. Intern. Med.* **2010**, *267*, 54.
[12] L. E. Freed, G. C. Engelmayr, M. Y. Cheng, C. J. Bettinger, J. T. Borenstein, R. Langer, *Nat. Mater.* **2008**, *7*, 1003.
[13] S. J. Lee, J. S. Choi, G. J. Christ, A. Atala, J. J. Yoo, *Biomaterials* **2008**, *29*, 2899.
[14] S. Li, K. Kurpinski, J. Chu, C. Hashi, *Proc. Natl. Acad. Sci. USA* **2006**, *103*, 16095.
[15] E. K. F. Yim, E. M. Darling, K. Kulangara, F. Guilak, K. W. Leong, *Biomaterials* **2010**, *31*, 1299.
[16] M. J. Dalby, N. Gadegaard, R. Tare, A. Andar, M. O. Riehle, P. Herzyk, C. D. W. Wilkinson, R. O. C. Oreffo, *Nat. Mater.* **2007**, *6*, 997.
[17] M. Yamato, O. H. Kwon, M. Hirose, A. Kikuchi, T. Okano, *J. Biomed. Mater. Res.* **2001**, *55*, 137.
[18] B. C. Isenberg, Y. Tsuda, C. Williams, T. Shimizu, M. Yamato, T. Okano, J. Y. Wong, *Biomaterials* **2008**, *29*, 2565.
[19] J. Y. Wong, C. Williams, Y. Tsuda, B. C. Isenberg, M. Yamato, T. Shimizu, T. Okano, *Adv. Mater.* **2009**, *21*, 2161.
[20] H. Takahashi, M. Nakayama, K. Itoga, M. Yamato, T. Okano, *Biomacromolecules* **2011**, *12*, 1414.
[21] C. W. Spancake, D. O. Kildsig, A. K. Mitra, *Pharm. Res.* **1991**, *8*, 345.
[22] E. Cho, J. S. Lee, K. Webb, *Acta Biomater.* **2012**, *8*, 2223.
[23] J. S. Tan, D. E. Butterfield, C. L. Voycheck, K. D. Caldwell, J. T. Li, *Biomaterials* **1993**, *14*, 823.
[24] I. Jun, K. M. Park, D. Y. Lee, K. D. Park, H. Shin, *Macromol. Res.* **2011**, *19*, 911.
[25] K. M. Park, I. Jun, Y. K. Joung, H. Shin, K. D. Park, *Soft Matter* **2011**, *7*, 986.
[26] Y. Yeo, W. L. Geng, T. Ito, D. S. Kohane, J. A. Burdick, M. Radisic, *J. Biomed. Mater. Res. B* **2007**, *81B*, 312.
[27] C. H. Chen, C. C. Tsai, W. S. Chen, F. L. Mo, H. F. Liang, S. C. Chen, H. W. Sung, *Biomacromolecules* **2006**, *7*, 736.
[28] Y. Liu, W. L. Lu, H. C. Wang, X. Zhang, H. Zhang, X. Q. Wang, T. Y. Zhou, Q. Zhang, *J. Controlled Release* **2007**, *117*, 387.
[29] Q. Zhou, Z. Zhang, T. Chen, X. Guo, S. B. Zhou, *Colloid Surf. B* **2011**, *86*, 45.
[30] J. A. Reed, A. E. Lucero, M. A. Cooperstein, H. E. Canavan, *J. Appl. Biomater. Biomech.* **2008**, *6*, 81.
[31] E. B. Biazar, E. M. T. Khorasani, M. Daliri, *Int. J. Nanomed.* **2011**, *6*, 295.
[32] F. Qiu, Y. Z. Chen, J. Q. Cheng, C. Wang, H. Y. Xu, X. J. Zhao, *Macromol. Biosci.* **2010**, *10*, 881.
[33] O. Guillaume-Gentil, Y. Akiyama, M. Schuler, C. Tang, M. Textor, M. Yamato, T. Okano, J. Voros, *Adv. Mater.* **2008**, *20*, 560.
[34] H. Obokata, M. Yamato, S. Tsuneda, T. Okano, *Nat. Protocols* **2011**, *6*, 1053.
[35] P. R. A. Kumar, H. K. Varma, T. V. Kumary, *Biomed. Mater.* **2007**, *2*, 48.
[36] P. S. Zammit, T. A. Partridge, Z. Yablonka-Reuveni, *J. Histochem. Cytochem.* **2006**, *54*, 1177.
[37] S. Li, N. F. Huang, S. Patel, R. G. Thakar, J. Wu, B. S. Hsiao, B. Chu, R. J. Lee, *Nano Lett.* **2006**, *6*, 537.
[38] W. N. Bian, N. Bursac, *Biomaterials* **2009**, *30*, 1401.
[39] M. A. Lan, C. A. Gersbach, K. E. Michael, B. G. Keselowsky, A. J. Garcia, *Biomaterials* **2005**, *26*, 4523.
[40] J. S. Nakamuta, M. E. Danoviz, F. L. N. Marques, L. Dos Santos, C. Becker, G. A. Goncalves, P. F. Vassallo, I. T. Schettert, P. J. F. Tucci, J. E. Krieger, *PLoS One* **2009**, *4*,
[41] W. Y. Lee, H. J. Wei, W. W. Lin, Y. C. Yeh, S. M. Hwang, J. J. Wang, M. S. Tsai, Y. Chang, H. W. Sung, *Biomaterials* **2011**, *32*, 5558.
[42] H. Obokata, M. Yamato, J. Yang, K. Nishida, S. Tsuneda, T. Okano, *J. Biomed. Mater. Res. A* **2008**, *86A*, 1088.
[43] T. Sasagawa, T. Shimizu, S. Sekiya, Y. Haraguchi, M. Yamato, Y. Sawa, T. Okano, *Biomaterials* **2010**, *31*, 1646.
[44] J. I. Lee, R. Nishimura, H. Sakai, N. Sasaki, T. Kenmochi, *Cell Transplant.* **2008**, *17*, 51.